IEEE Access
Multidisciplinary ⋮ Rapid Review ⋮ Open Access Journal

Received 4 March 2025, accepted 13 March 2025, date of publication 26 March 2025, date of current version 7 April 2025.

Digital Object Identifier 10.1109/ACCESS.2025.3554744

RESEARCH ARTICLE

Lung-AttNet: An Attention Mechanism-Based CNN Architecture for Lung Cancer Detection With Federated Learning

CHAMAK SAHA[1], SOMAK SAHA[2], MD. ASADUR RAHMAN[3], (Student Member, IEEE), MD. MAHMUDUL HAQUE MILU[4], HIROKI HIGA[5], MOHD ABDUR RASHID[6], AND NASIM AHMED[7], (Senior Member, IEEE)

[1]Department of Animal and Dairy Science, University of Georgia, Athens, GA 30602, USA
[2]Department of Computer Science and Engineering, BRAC University, Dhaka 1212, Bangladesh
[3]Department of Biomedical Engineering, Military Institute of Science and Technology (MIST), Dhaka 1216, Bangladesh
[4]Department of Biomedical Engineering, Jashore University of Science and Technology (JUST), Jashore 7408, Bangladesh
[5]Department of Electrical and Electronics Engineering, University of the Ryukyus, Okinawa 903-0213, Japan
[6]Department of EEE, Noakhali Science and Technology University, Noakhali 3814, Bangladesh
[7]School of Computer Science, The University of Sydney, Sydney, NSW 2006, Australia

Corresponding author: Nasim Ahmed (nasim.ahmed@sydney.edu.au)

ABSTRACT Lung cancer is one of the fatal diseases whose early diagnosis is essential to mitigate the death rate. Computed Tomography (CT) scans are widely used for lung cancer diagnosis, but manual interpretation by health professionals can lead to inconsistent results. To address this, we propose Lung-AttNet, a novel lightweight convolutional neural network (CNN) model enhanced with an attention mechanism. Lung-AttNet incorporates a convolutional block with a Lightweight Global Attention Module (LGAM) to effectively distinguish between lung cancer types. The convolutional block extracts both low- and high-dimensional features, while LGAM captures feature dependencies across channel and spatial dimensions. The model is evaluated using the Kaggle CT scan dataset, which includes four classes: adenocarcinoma, large cell carcinoma, squamous cell carcinoma, and normal. Extensive experiments, including ablation studies, 5-fold cross-validation, and explainable AI (XAI) techniques such as Grad-CAM and LIME, demonstrate that Lung-AttNet achieves an average accuracy of 91.5%. Furthermore, to address medical data sensitivity and privacy concerns, the model is deployed in a Federated Learning (FL) framework, where the global model is trained using weights from local models rather than sharing raw data. In the FL environment, Lung-AttNet achieves an accuracy of 92% with 2 and 3 clients, underscoring its robustness and adaptability for real-world applications.

INDEX TERMS CNN, LGAM, federated learning, XAI, Lung-AttNet.

I. INTRODUCTION

Cancer is a severe global health concern with rising mortality rates every day. Among different cancer types, lung cancer is deadlier because it has a higher fatality rate [1]. Every year the growth of lung cancer patients is increasing in numbers gradually and its survival rate is the lowest after the diagnosis of the patients [2]. Depending upon cellular characteristics, lung cancer has two types. One is non-small cell lung cancer and the other is small cell lung cancer. On top of that, there are four stages of lung cancer. Lung cancer is often identified in the last stages, which makes the treatment procedure more problematic and challenging and it drastically reduces the survival rate [3]. If the cancer is identified early, it increases the patient's survival rate significantly [4]. So, it is essential to detect cancers in earlier stages efficiently. Computed Tomography (CT) scan images are considered the most prominent in lung cancer diagnosis. By analyzing the anomalies in the CT scan images, physicians determine whether a patient is lung cancer-affected or not.

The associate editor coordinating the review of this manuscript and approving it for publication was Wei Ni.

In the recent past, computer-aided biomedical applications have been used frequently in several disease diagnosis [5]. In the medical sector, the trend of preserving patient data has greatly increased. Therefore, deep learning-based medical diagnosis systems are well known [6]. Recently, in lung cancer diagnosis, image processing-based techniques have been utilized to identify the lung condition efficiently. Several studies relied on Deep Convolutional Neural network (DCNN) based architectures because CNN enables automatic feature extractions that traditional machine-learning algorithms lack [7], [8]. Transfer learning approaches also utilize the CNN models to work proficiently in small datasets. CNN and Transfer learning models however struggle to perform decently to distinguish the class of the medical image when the inter-class similarity is high [9]. Pre-trained CNN architectures and vanilla CNN models additionally do not have any built-in attention mechanism to figure out explicit important and unimportant features. Most recent studies on lung cancer diagnosis take place in a centralized environment, where the challenge of limited sample size often arises when working within a single institution or center [10]. One direct solution could be building a larger centralised diverse dataset by acquiring data from different centers. Due to sensitivity and privacy protection issues, though, medical data sharing is unfeasible from one center to another to develop a quality AI model. It breaches the law of data confidentiality and data governance [11], [12]. Most of the image-based lung cancer diagnosis studies, also, could not provide much visual explainability of their produced results to make their suggested models (black box model) trustworthy. Therefore, there is enough room for improvement in lung cancer diagnosis especially,

- To capture explicit feature importance distinguishing high inter-class similarity-based images.
- To preserve data privacy and protection.
- To provide the interpretability of the model's performance.

Considering the factors above, this study proposes a lightweight attention mechanism-based CNN architecture to diagnose lung cancer. Integrating different attention modules in the proposed model helps to select explicit relevant features and suppress unimportant information [13]. It could help to classify images when inter-class similarity is high. On top of that, the model is trained in both a centralized and decentralized environment. Federated Learning (FL) technology has been adopted to train the model in a decentralized environment that considers data protection and privacy. In a FL environment, model distribution/ aggregation/ fusion is performed to train a global model without exchanging data [14]. A couple of Explainable AI techniques are also used to provide the interpretation of the produced results of the proposed model. To summarize the main contributions of the study are:

- A custom lightweight attention mechanism-focused deep learning model called Lung-AttNet is introduced to classify lung cancer. In the proposed Lung-AttNet, a convolution block is integrated with a lightweight global attention module (LGAM) to diagnose lung cancer appropriately.
- To enhance the image quality, white balancing and CLAHE techniques are performed in image preprocessing.
- Considering the privacy protection issues of the data, this research is conducted in both a centralized and decentralized environment. To adopt model training in a decentralized environment, the Federated Learning technique is utilized to preserve patient data protection.
- Utilization of the 5-fold cross-validation technique is made to generalize the model's produced results. Besides, two Explainable AI methods, Grad-CAM and LIME are applied to provide the visual interpretability of the produced results of Lung-AttNet.

After extensive experiments along with ablation studies, it was found that the proposed Lung-AttNet model obtained an accuracy of 91.5% in the centralized environment and 92% in the decentralized environment.

The remaining of the paper is as follows. Section II provides a description of the literature review which is followed by methodology in Section III. Section IV discusses the findings of the study while Section V gives the conclusion.

II. LITERATURE REVIEW

In detecting lung cancer, several studies have been conducted to develop computer-aided diagnosis systems to make the diagnosis system autonomous. Among them, most of the systems are based on deep learning architecture where CNN-based approaches are most preferred in CT scan image analysis. A thorough analysis of the prior work is beyond the scope of the paper, however, a short description of the related works is given below:

This study [15] presented a hybrid CNN-based approach to classify lung cancer from CT images. Initially, to get better performance the authors did data augmentation. Then, they applied AlexNet, LeNet, and VGG16 to extract features and used several machine-learning classifiers for classification tasks. After performance evaluation, it was found that AlexNet and KNN classifier performed best (98.74% accuracy).

To predict lung cancer from CT scan images, the authors [16] proposed a model integrating XGBoost and MobileNet where XGBoost is used for feature extraction and MobileNet performs the classification task. Besides, they developed a web application to identify lung cancer from CT scan images. In the data preprocessing stage, apart from the resizing images, they did not mention any specific task. Point to mention that, in the research, they did not perform any cross-validation for generalizing the proposed model in real-life application.

In the research, the author [17] applied several pre-trained models including VGG16, VGG19, ResNet50, and

DenseNet201 to classify lung cancer from CT scan images. Among different models, VGG16 performed very decent. It is noteworthy to mention that a comprehensive analysis of combining different image enhancement techniques was an important contribution of the research where the combination of CLAHE and Unsharp Masking (USM) was superior in performance. The issue to note is that they did not use XAI methods to bring the explainability of the black box models. Also, cross-validation was missing for the generalization of the models.

Saric et al. [18] followed CNN based approach to detect lung cancer. They applied VGG16 and ResNet50 to classify lung cancer from whole slide images. In the result analysis, it was found 75.4% and 72.1% accuracy for VGG16 and ResNet50 respectively. In parallel, Al-Yasriy et al. [19] also used Pre-trained CNN architectures. Using CT scan dataset collected from Iraqi hospitals, they applied AlexNet to classify lung cancer. Besides, this study [20] compared the performance of LeNet, ResNet, and AlexNet to detect lung cancer. In performance analysis, it was found that ResNet performed better. Similarly, Vij and Kaswan [21] implemented VGG16.

To detect lung cancer, this study [22] proposed a custom CNN model. On top of that, the proposed model was compared with 3 pre-trained models such as ResNet50, InceptionV3, and Xception. Using Kaggle CT scan data, it was observed that their proposed model performed better than the pre-trained architectures in several evaluation metrics. Similarly, the authors [23] presented an automatic lung cancer detection system using CNN. Their proposed model performed well and it obtained 97.2% accuracy.

Sajja et al. [24] proposed a transfer learning-based approach. In their work, they designed a CNN model based on GoogleNet. Besides, they used dropout layer to reduce the overfitting issues. Also, they compared their proposed model with pre-trained CNN models including ResNet50, AlexNet, and GoogleNet. In the result analysis, it was observed that their proposed model performed better than pre-trained models. Similarly, Bhola et al. [25] and Lathakumari et al. [26] utilized EfficientNet B2 for lung cancer detection from CT scan images. It obtained 90.16% and 83% accuracy respectively. Similarly, Shah et al. [27] tried to find a solution to detect lung cancer using 2D CNN. In their study, initially, they built 3 custom CNN models and trained the models using CT scan data. Then, they combined the results of 3 CNN models using ensemble approaches. Their proposed ensemble model performed well and it obtained 95% accuracy.

Swain et al. [28] opted for InceptionV3 for its less complex architecture to identify lung cancer types. Using the LC25000 dataset the research was conducted in two phases such as feature extraction and classification of the type of cancer. In performance analysis, it was found that the proposed model (InceptionV3) surpassed comparatively complex CNN models VGG19 and ResNet50.

Shatnawi et al. [29] developed a custom CNN architecture for detecting lung cancer. Histogram equalization and data augmentation methods were followed to improve the model performance. The proposed model found better evaluation performance than the transfer learning models. Similarly, Hangaragi et al. [30] proposed a convolutional autoencoder (CA) for generating synthetic samples of lung cancer. Then, the synthetic samples were combined with the existing database. Later the combined augmentation data were passed to CNN architecture for the classification of lung cancer. The key contribution of this research was that the CA-based augmentation dataset provided better outcomes than the traditional augmentation-based augmentation dataset.

The authors [31] proposed a hybrid CNN-LSTM approach where CNN was used for feature extraction and LSTM performed the classification task. In the research, the author utilized the segmentation of images through the (OTSU) thresholding method. Besides, they used the median filter to remove the unwanted noise from CT scan images.

The study [32] suggested the DCNN-GRU model for accurate classification of lung abnormalities. In their proposed model, the incorporation of the GRU layer contributed to reducing training time because the GRU layer had fewer parameters. One of the key aspects of the research is that they used multiple XAI techniques to provide an interpretation of the produced results of the proposed model. Similarly, the research [33] focused on introducing an XAI-based machine-learning model to predict the risk of lung cancer caused by pesticide exposure. The SMOTE and ENN combined hybrid technique was utilized to tackle the class imbalance of the dataset. XGBoost Classifier was implemented for the prediction and the SHAP method was used for performance interpretation.

The authors [34] designed a robust feature extraction-capable vision transformer model called FocalNeXt. In FocalNeXt, ConvNeXt was incorporated into the FocalNet architecture. The core significance of FocalNeXt was that through extensive experiments combined with ablation study, and comprehensive evaluation, it was found that it surpassed several SOTA ViT models.

The mentioned papers above focused on centralized data and model performance, with little attention to data security. A few explored lung cancer detection using federated learning to preserve data sensitivity in decentralized environments.

In the proposed methodology [35], to preserve the privacy of the patient's data, the authors introduced a federated learning framework combined with CNN to diagnose lung disease. The performance of the FL-CNN model was comprehensive having an accuracy of 99% across various healthcare centres and diverse lung illnesses. Besides, the model showed its effectiveness against the unbalanced dataset which strengthens its generalizability. In parallel, this study [36] presented a framework for the privacy protection of data that integrated federated learning and CNN to diagnose lung diseases from X-ray images. In this research, the authors proposed a custom CNN architecture for deploying in the federated learning environment. Besides, the model dealt with 5 different classes of lung diseases among 5 separate

TABLE 1. Comparative summary of the literature review.

Study	Method	Attention Mechanism Used	XAI Used	Security	Cross Validation Used	Limitations
Shah et al. [27]	CNN	No	No	No	No	1.Model fine-tuning is missing 2.Lack of image enhancement technique
Mamun et al. [22]	CNN	No	No	No	No	1.Ablation Study is missing 2.Lack of image enhancement technique
Abdul [23]	CNN	No	No	No	No	1.Image preprocessing missing 2.Model fine-tunning is missing
Saric et al. [18]	CNN	No	No	No	No	1.Lack of experiment
Al-Yasriy et al. [19]	CNN, AlexNet	No	No	No	No	1.Lack of experiment
Chitale et al. [16]	XGBoost-MobileNet	No	No	No	No	1.Ablation study is missing 2.Lack of image enhancement technique
Al-areqi et al. [17]	VGG16, VGG19, ResNet50, DenseNet201	No	No	No	No	1.Ablation study is missing
Swain et al. [28]	Inception V3, VGG16, ResNet 50	No	No	No	Yes	-
Islam et al. [32]	DCNN-GRU	No	Yes	No	No	-
Islam et al. [37]	DCNN-ViT-GRU	Yes	Yes	No	Yes	-
Jindal et al. [36]	CNN	No	No	Yes	No	1.Image enhancement is missing
Jindal et al. [35]	CNN	No	No	Yes	No	1.Image enhancement is missing
This study	**Proposed Lung-AttNet (CNN+LGAM)**	**Yes**	**Yes**	**Yes**	**Yes**	-

customers (clients). Analyzing the data from different sources the model achieved very decent performance in accuracy.

Also, Palash and Yousuf [38] followed some transfer learning methods for lung cancer detection with a combination of Federated Learning to address data privacy concerns. In the initial phase, different transfer learning CNN models were trained and among them, MobileNet V2 provided better output. Then FL (two clients) was implemented on MobileNetV2.

The study [39], proposed a survival prediction model for lung cancer patients using routine radiation oncology data. Federated Learning was used for data collection. Logistic Regression was performed for model training and validation. Feature selection was performed through univariate sand model-based analysis, with bootstrapping for optimization. Similarly, to detect lung cancer from CT scan images, the authors [40], proposed a novel FBCLC-Rad framework which is a combination of federated learning and blockchain technology. Federated learning ensures the training of a global deep learning model from different hospitals while maintaining data privacy and blockchain offers data authenticity. In this research, data normalization was used to enhance the performance. In the result evaluation, FBCLC-Rad performed very decent in detecting lung cancer and surpassed state-of-the-art methods. Besides, to detect lung nodules efficiently, the authors [41] introduced a novel model, 3D ResNet18 dual path Faster R-CNN. They deployed the model in a federated learning environment where the Fed Average algorithm was used. Besides, to mitigate overfitting issues and for better generalization, the author introduced a sampling-based content diversity algorithm. In evaluation, the proposed method performed quite well while maintaining data privacy. Similarly, the study [42], [43] deployed several transfer learning models in the FL environment to detect lung cancer from microscopy and histopathological images respectively.

Babar et al. [44] presented a Federated Active Learning with a Transfer Learning framework to address data annotation challenges in lung cancer diagnosis while preserving patient privacy. Using ensemble entropy-based uncertainty assessment and transfer learning, FAL-TL optimized annotation and outperformed traditional models.

The literature survey shows that most of the study was conducted using CNN and Transfer Learning approaches, which failed to figure out explicit feature importance. Therefore, there is much scope to work on in this context. Also, only a few studies focused on the model's performance visual explainability. Most of the study conducted research in a centralized environment which awakens the issue of data privacy shown in TABLE 1. Considering these issues, this

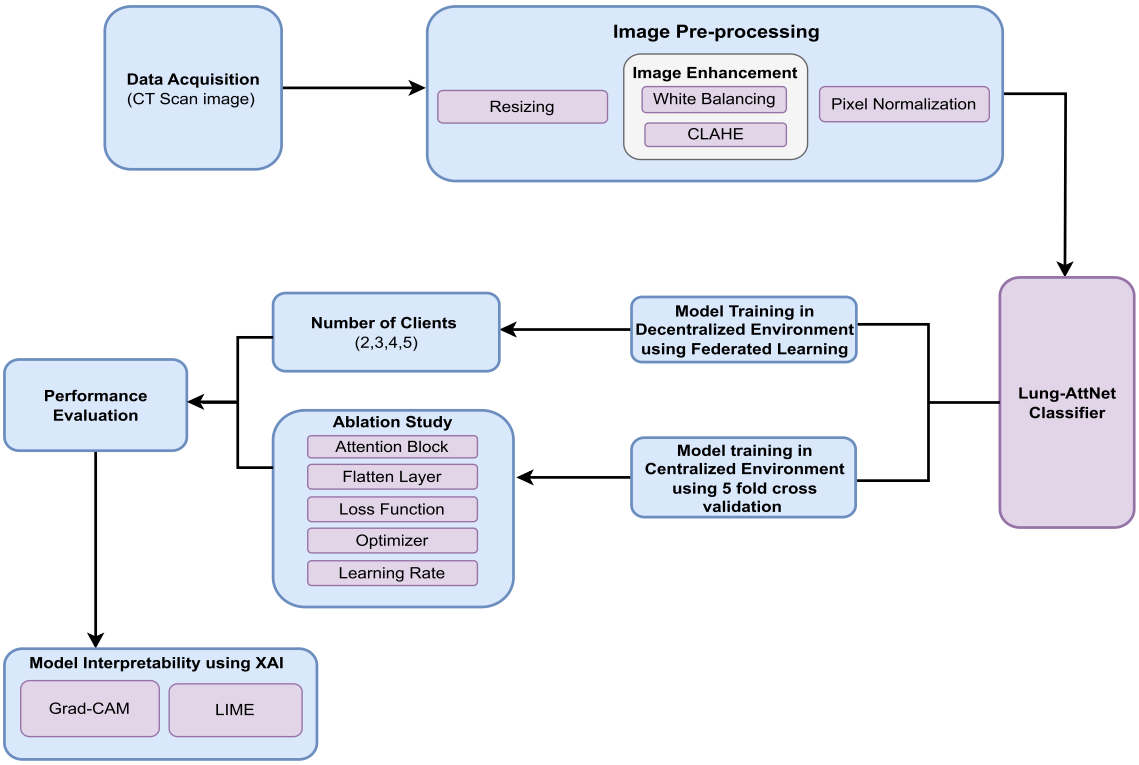

FIGURE 1. Top-level overview of the research.

study focuses on designing a multiple-attention mechanism (LGAM) driven unique CNN architecture for lung cancer diagnosis integrated with Federated Learning and XAI.

III. METHODOLOGY

As shown in Figure. 1, the research is conducted in both a centralized environment and a decentralized environment. Both of the scenarios are separated into multiple segments including data acquisition, image preprocessing, Lung-AttNet Classifier, performance evaluation, and model interpretation via XAI. The following subsections and sections are going to discuss each of them.

A. DATASET DESCRIPTION

To accomplish the research, Computed Tomography (CT) scan data of lung cancer is collected from Kaggle [45]. The dataset consists of a total of 1000 images of four classes: Adenocarcinoma, Large Cell Carcinoma, Squamous Cell Carcinoma, and Normal (not lung cancer) shown in Figure. 2, and the detailed description is given in the TABLE 2.

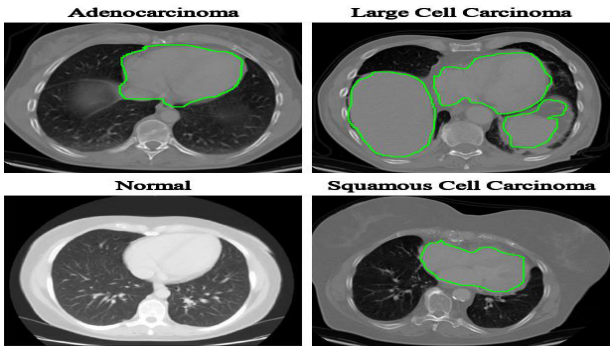

FIGURE 2. Samples of the Dataset.

TABLE 2. Description of the dataset.

Name of the class	Number of images
Adenocarcinoma	338
Large Cell Carcinoma	187
Squamous Cell Carcinoma	260
Normal	215

B. DATA PRE-PROCESSING

To improve the performance of the proposed model, data preprocessing is required. Initially, images are resized into $224\times224\times3$ dimensions. After that, white balancing and CLAHE utilization are performed for the sake of image enhancement shown in Figure. 3.

Due to variations in the lighting conditions, the color of the image becomes undesirable. White balancing is a method that enhances the quality and color of the image. Using white balancing, the image's color adjustment is processed to correct the color cast.

Contrast limited adaptive histogram equalization (CLAHE) technique is an improved version of the adaptive histogram equalization (AHE).It boosts the local contrast of the image along with its usability. Besides, by preventing noise amplification CLAHE enhances the clarity, sharpness, and visibility of the image. It can calculated as:

$$G(i,j) = \frac{L-1}{MN} \sum_{k=0}^{i} \sum_{i=0}^{j} p(f(k,l), C) \tag{1}$$

Here, G(i,j) defines enhanced image pixel value, L represents intensity levels, M and N are image dimensions, p(f(k,l)) is the cumulative distribution function of the pixel intensities, C represents the clipping threshold. In the CLAHE technique, both tile size and clip limit are influential hyperparameters. In this research, clip limit (2.0), and tileGridSize (16, 16) are chosen. Lastly, pixel normalization is used.

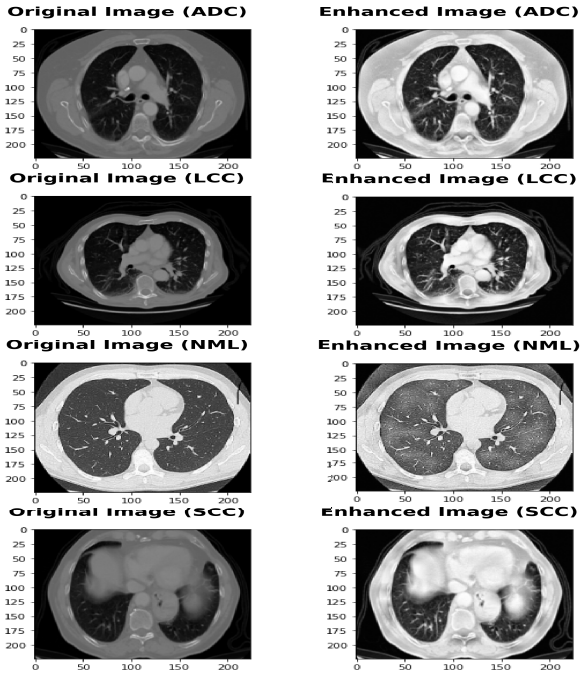

FIGURE 3. Sample image after performing White Balancing and CLAHE processing: ADC (Adenocarcinoma), LCC (Large Cell Carcinoma), NML (Normal), SCC (Squamous Cell Carcinoma).

IV. PROPOSED LUNG-ATTNET

In this research, a novel attention mechanism-oriented deep learning model called Lung-AttNet is designed to detect lung cancer shown in Figure. 4. In the architecture of Lung-AttNet, there are mainly 2 components such as convolution block, and LGAM. In Lung-AttNet, the convolution block enables the model to extract both high and low-dimensional features. In the model, LGAM [9] is utilized to figure out the feature dependencies in channel and spatial dimensions (Figure. 5).

A. CONVOLUTION BLOCK

The preprocessed input image is passed into the convolution block which consists of 4 Conv2D layers (kernel size=3) to extract the low and high level features. In between the convolution layers, the Max pooling or Average pooling layers (size=2) are used for achieving translation invariance and reducing computation complexity. The Relu activation function is introduced in the network to bring nonlinearity and also to alleviate the vanishing gradient problem.

The output feature is later passed to the lightweight global attention module.

B. LIGHTWEIGHT GLOBAL ATTENTION MODULE (LGAM)

In the proposed model, LGAM is comprised of three types of attention mechanisms where Spatial attention and Self-attention are structured in parallel to generate an attention map from the spatial relationship in the feature map. Then, to figure out the inter-channel dependencies of the merged attention map generated by Spatial attention and Self-attention is passed to the channel attention module. The following subsection will discuss each attention block in detail.

C. SPATIAL ATTENTION BLOCK

Along spatial dimensions, to emphasize the inter-feature dependencies of the lung cancer images, a Spatial Attention Block (SAB) is incorporated. The input feature $F \in \mathbb{R}^{H\times W\times C}$ of the LGAM module is passed to the SAB where both max pooling and average pooling operations are used to create feature maps F_1,F_2. Then both of the feature maps F_1 and F_2 are concatenated, and the Relu activation function is used which generates the intermediate output F'.

$$F' = \text{ReLU}\left(\text{concat}\left(\text{AvgPool}(F), \text{MaxPool}(F)\right)\right) \tag{2}$$

The output F' is then passed to the Conv layer with kernel size 1 (sigmoid activation function) to create the attention map. Lastly, the attention map is multiplied by the input.

$$F_{sab} = \sigma(\text{conv}_{1\times1}(F')) \odot F \tag{3}$$

Here, σ and $\odot$ represent the sigmoid activation and element-wise multiplication respectively.

D. SELF-ATTENTION BLOCK

To compute the long-range dependencies in the images self-attention is introduced in the model. Self-attention enables the model to capture a wide range of multi-level feature dependencies across the regions of the images. Initially, input feature $F \in \mathbb{R}^{H\times W\times C}$ is passed through Conv layers and generates 3 transformed feature maps: $\hat{F}_1 \in \mathbb{R}^{H\times W\times C'}$, $\hat{F}_2 \in \mathbb{R}^{H\times W\times C'}$, $\hat{F}_3 \in \mathbb{R}^{H\times W\times C'}$, where $C' = C/8$ is decided empirically. Then, transformed feature maps are reshaped into $\mathbb{R}^{M\times C'}$, where M=H*W. Then cross product is performed between $\hat{F}_1$ and $\hat{F}_2$ (transpose) to create an attention map. Further, the Softmax is used to normalize

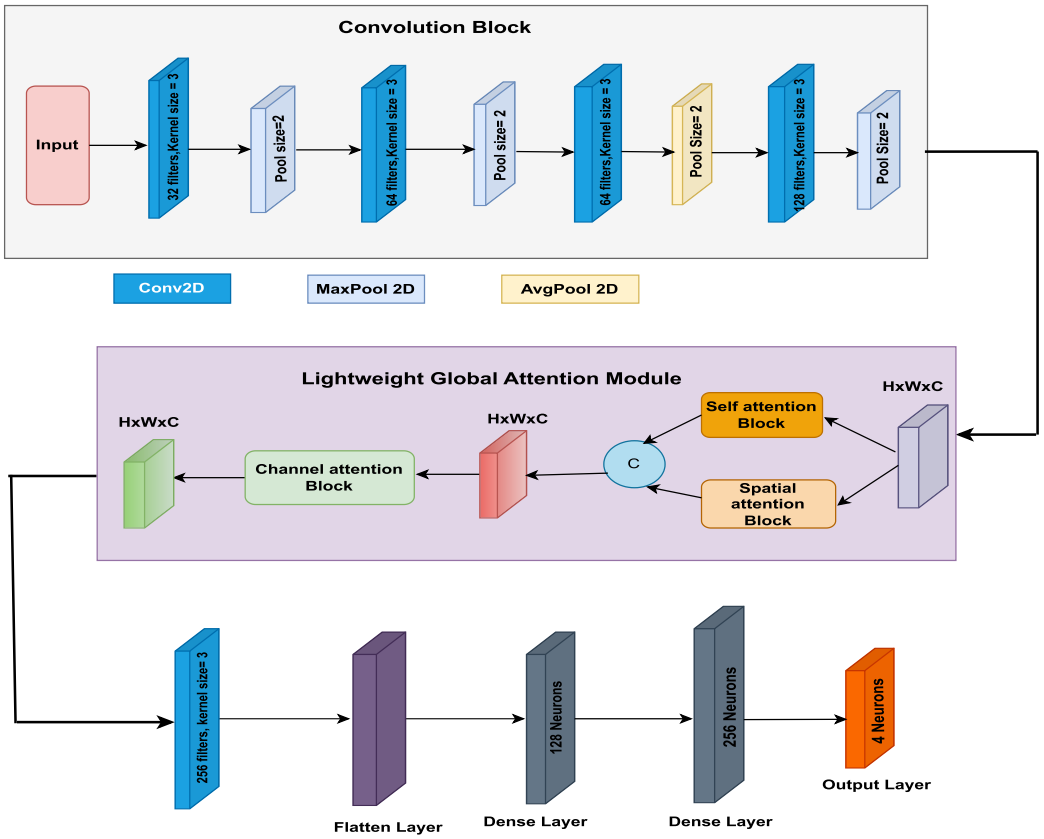

FIGURE 4. Architecture of the proposed Lung-AttNet.

the attention map which is later multiplied with the $\hat{F}_3$ and reshaped. Finally, a Conv layer (kernel=1) followed by ReLU activation is used for generating attention-wise feature maps.

$$\bar{\mathbf{F}}'_s = \Phi(\hat{\mathbf{F}}_1 \otimes \hat{\mathbf{F}}_2^T) \tag{4}$$

$$\mathbf{F}_{sb} = ReLU(\text{conv}_{1\times1}(\bar{\mathbf{F}}'_s \otimes \hat{\mathbf{F}}_3)) \tag{5}$$

Here, ϕ and $\otimes$ define the softmax activation and matrix multiplication respectively.

E. AGGREGATION

Through addition, the generated feature maps by the SAB and SB (Self Attention Block) are combined and passed to the Channel Attention Block.

$$F_{\text{agg}} = F_{\text{sab}} \oplus F_{\text{sb}} \tag{6}$$

F. CHANNEL ATTENTION BLOCK

To compute the channel-wise feature dependencies of the resultant attention-wise feature maps created by aggregating SAB and SB, a Channel Attention Block (CAB) is introduced. In CAB initially, the global max pooling operation is applied on the aggregated input feature map. Later, the output of the global max pool operation is passed to the following two Conv layers with kernel size 1 (Relu and Sigmoid activation function respectively) to create the channel-wise attention map. Lastly, the attention map is multiplied by the input to generate an attention-wise feature map.

$$F_{cab} = \sigma\left(\text{Conv}_{1\times1}\left(\text{ReLU}\left(\text{Conv}_{1\times1} \times \left(\text{GMP}\left(F_{\text{agg}}\right)\right)\right)\right)\right) \odot F_{\text{agg}} \tag{7}$$

The output of the LGAM is then passed to a Conv2D layer. Next, the output of the Conv2D layer is flattened and passed to 2 consecutive Dense layers of 128 and 256 neurons respectively. Lastly, the output layer (4 neurons) is used to classify the images of lung cancer. The optimal training configuration of the proposed Lung-AttNet is represented in TABLE 3.

TABLE 3. Training configuration of proposed Lung-AttNet in both centralized and decentralized environments.

	Centralized Environment	Federated Learning Environment
Parameter	3.749 M	3.749 M
Optimizer	Nadam	SGD
Learning rate	0.001	0.001
Epoch	30	30
Loss Function	Categorical Cross Entropy	Categorical Cross Entropy
Communication Round	-	10

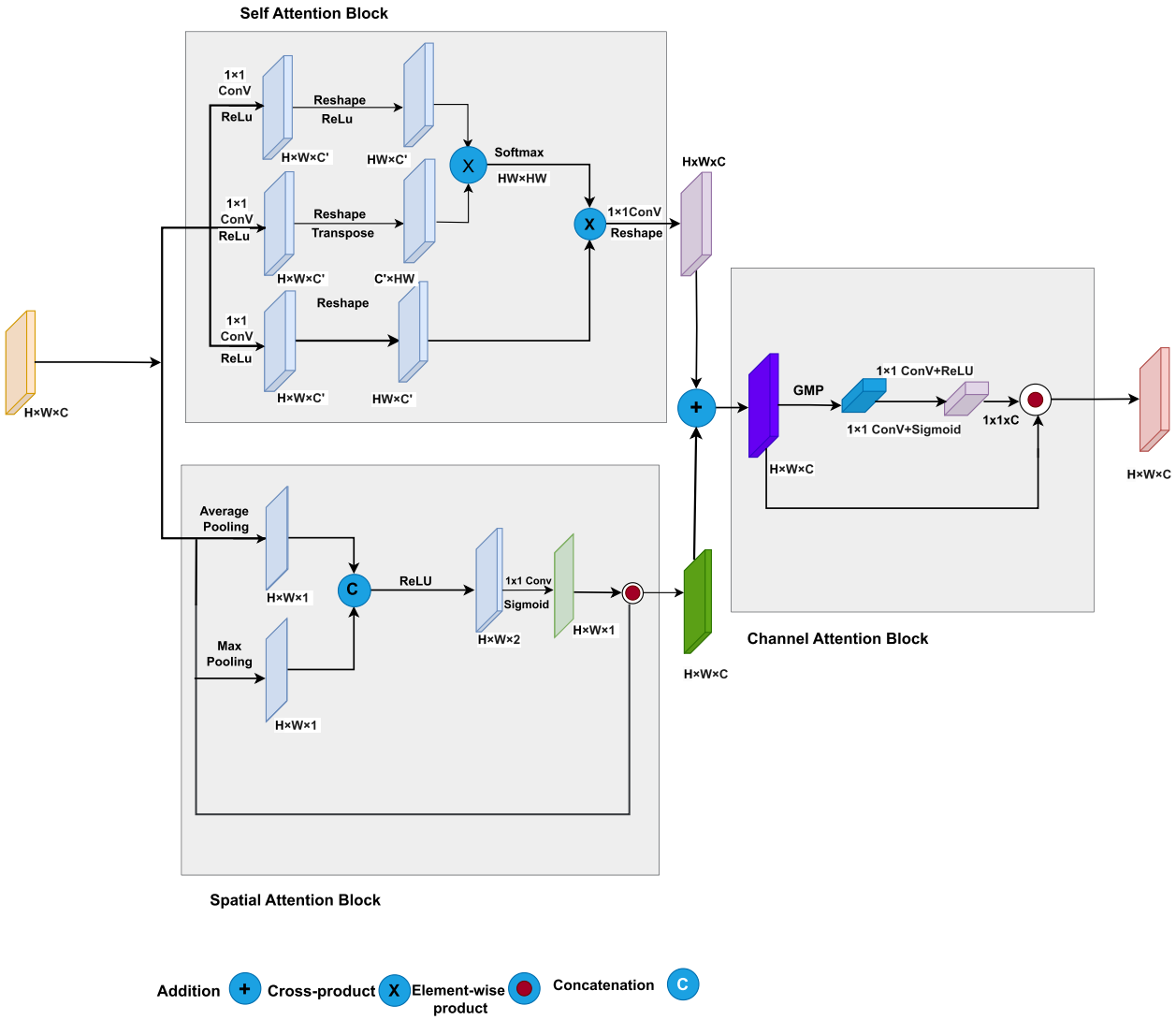

FIGURE 5. Architecture of LGAM.

G. FEDERATED LEARNING

Federated Learning is an emerging technology which addresses the issue of data confidentiality shown in Figure 6. In medical image analysis, FL plays a vital role in bringing patient diversity and preserving data security [46], [47]. In FL there are two ends such as the central server (global server) and the client end (local server). The global server consists of the global model and local servers store the client data from the end users or devices. In the FL environment model training is performed in decentralized devices without sharing client data. In such a scenario, the global model looks for information from the clients where the clients have established a connection with the global model. The client does local model training using local data, and then, it sends the information of weight changes to the global model without sharing data. After receiving all the updates from the local models the global model combines them using the FedAvg method shown in the equation.

$$p^g_{t+1} = \frac{1}{c_i} \sum_{i=1}^{c_i} \delta_i \cdot p^i_t \tag{8}$$

Here, p^g_{t+1} defines the global model update during the time (t+1), and c_i is the number of clients that participate in the averaging. δ_i defines the weights added to each client at the time of the averaging process and p^i_t represents the parameter of the local model at the time t on the device i.

H. FEDERATED LEARNING SETUP

1) OVERVIEW OF FEDERATED LEARNING PROCESS

In this study, the federated learning framework follows a client-server architecture where multiple clients (2,3,4,5) train local models on their respective data shards. These locally trained models contribute to the global model without

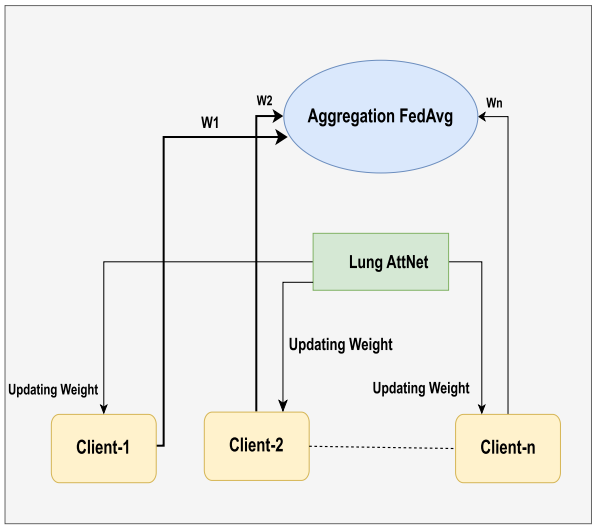

FIGURE 6. Federated Learning Framework for the proposed Lung-AttNet.

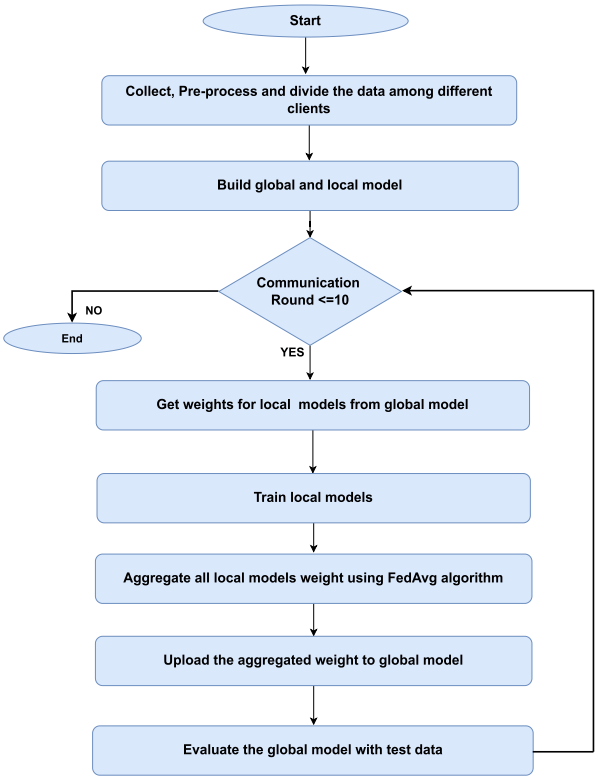

FIGURE 7. Flow chart of the FL system.

sharing raw data, ensuring privacy. The primary components of the FL environment include:

- **Clients:** Each client represents a distributed entity with its subset of training data.
- **Server:** The central entity aggregates the locally trained models and updates the global model.

2) DATA DISTRIBUTION AND CLIENT SETUP

The data distribution process ensures that each client receives a balanced subset of the overall dataset. The training data is partitioned among a specified number of clients. The data is randomly shuffled to ensure an unbiased distribution. Each client's data shard is processed into batches for efficient training using TensorFlow. The test set is batched separately to evaluate the global model at each communication round.

3) CLIENT-SERVER INTERACTION

The federated learning setup follows an iterative training process, involving multiple communication rounds between the server and clients (Figure. 7). The process is as follows:

- **Global Model Initialization:** The server initializes a global model using the lightweight CNN architecture with predefined layers and attention mechanisms.
- **Server:** The central entity aggregates the locally trained models and updates the global model.
- **Model Distribution to Clients:** At the beginning of each communication round, the server sends the current global model weights to all participating clients. Each client represents a distributed entity with its subset of training data.
- **Local Training at Clients:** Each client initializes a local model, loads the global weights, and trains on their local dataset for a fixed number of epochs.
- **Weight Scaling and Aggregation:** After local training, each client's model weights are scaled based on their data proportion to maintain fairness. The server aggregates the scaled weights to update the global model using Federated Averaging (FedAvg).
- **Global Model Evaluation:** After each communication round, the updated global model is tested on the centralized test set, and various performance metrics (accuracy, loss, precision, recall, F1-score, AUC) are recorded.

4) DATA INTEGRITY AND CONSISTENCY

To ensure the integrity and consistency of data across the federated learning pipeline, the following measures were taken including Shuffling and Batching, Weight Scaling for Fairness, and Clearing Sessions.

Federated learning inherently ensures privacy by keeping data local to clients. The raw data is never transmitted to the central server, as only model updates (weights) are exchanged. This is crucial for scenarios with sensitive data, such as medical imaging applications in the given context (lung cancer classification). The training process runs for a specified number of communication rounds allowing the global model to gradually converge by aggregating the knowledge from distributed clients. By implementing these mechanisms, the federated learning environment ensures efficient, fair, and privacy-preserving collaborative learning across distributed clients.

V. EXPERIMENTAL RESULTS AND DISCUSSION

To conduct this research, Intel Core i5 CPU with 8GB RAM is used. Accuracy, precision, recall, F1 score, and AUC are used to evaluate performance [48].

TABLE 4. Fold-wise performance evaluation of the proposed Lung-AttNet (Optimal configuration).

Fold	Accuracy(%)	Precision (%)	Recall (%)	F1 Score (%)	AUC (%)
Fold-1	92	92.4	92	92.07	98.99
Fold-2	91	91.37	91	90.97	98.95
Fold-3	92	92.19	92	92.08	99.15
Fold-4	92.5	92.6	92.5	92.48	99.45
Fold-5	90	89.9	90	89.9	98.17
Average	**91.5**	**91.69**	**91.5**	**91.48**	**98.94**

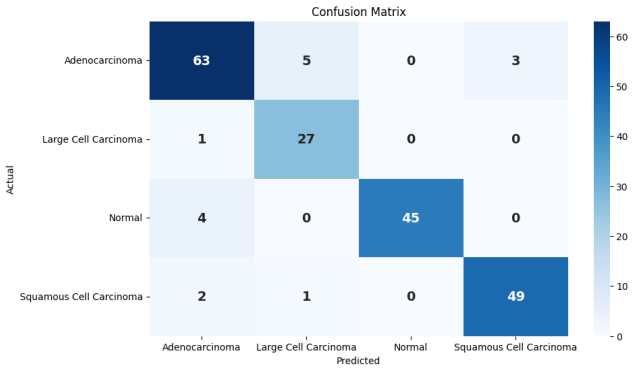

FIGURE 8. Confusion matrix for Fold 1.

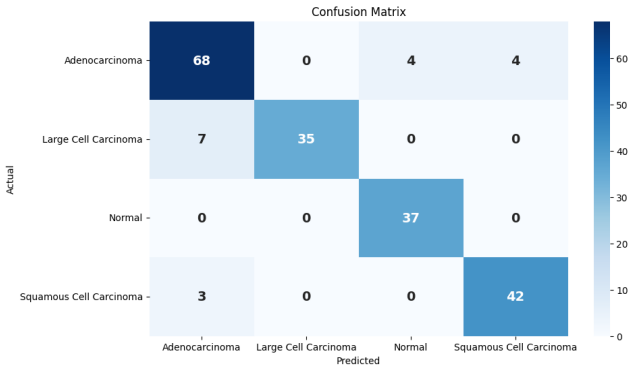

FIGURE 9. Confusion matrix for Fold 2.

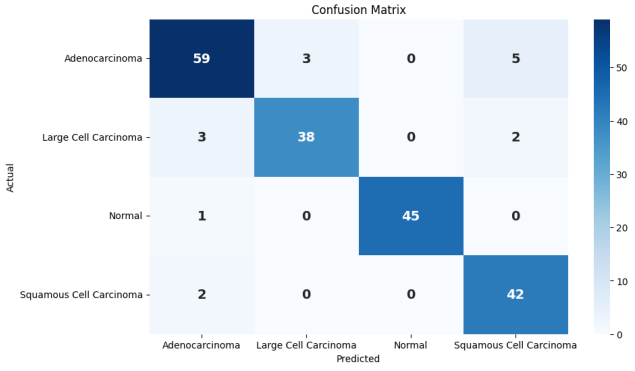

FIGURE 10. Confusion matrix for Fold 3.

The proposed Lung-AttNet model's performance in each cross-validation fold was notable. In each fold of the cross-validation, the proposed model obtained performance above 90% in all evaluation metrics and on average the proposed model achieved an accuracy of 91.5% (TABLE 4). The confusion matrix illustrating the performance of the proposed model on each fold of cross-validation is represented in the Figure. 8, Figure. 9, Figure. 10, Figure. 11, and Figure. 12.

The proposed Lung-AttNet performance varied when the learning rate changed. It provided the best outcomes when the learning rate was kept at 0.001 and the optimizer was Nadam shown in TABLE 5. It achieved an average accuracy of 91.5%. In terms of precision, recall, F1 score, and AUC, the proposed model obtained 91.69%, 91.5%, 91.48%, and 98.94%, respectively on average. The performance of Lung-AttNet lessened as the learning rate decreased. The proposed model performed poorly when the learning rate was 0.00001 (Nadam optimizer) and it achieved an average accuracy of 61.9%.

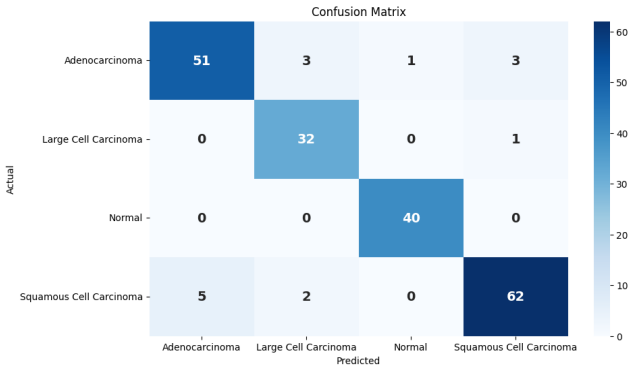

FIGURE 11. Confusion matrix for Fold 4.

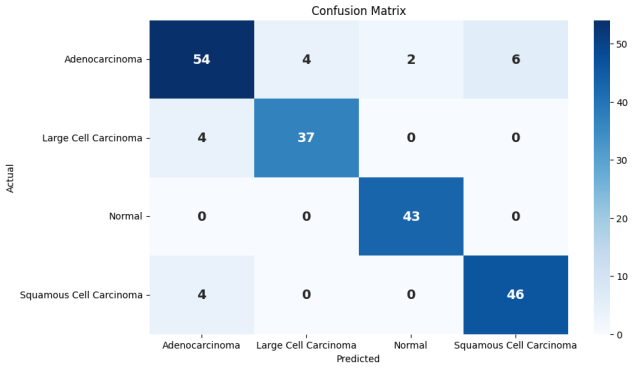

FIGURE 12. Confusion matrix for Fold 5.

TABLE 5. Ablation Study 1: Altering Learning Rate for different Optimizers.

Optimizer	Learning Rate	Average Accuracy(%)	Average Precision(%)	Average Recall(%)	Average F1 Score (%)	Average AUC(%)
Adam	0.001	89.8	90.02	89.8	89.76	98.34
	0.0001	87.9	88.71	87.9	87.92	98.39
	0.00001	61.5	66.03	61.5	60.3	86.17
Nadam	**0.001**	**91.5**	**91.69**	**91.5**	**91.48**	**98.94**
	0.0001	89.5	89.79	89.5	89.43	98.44
	0.00001	61.9	65	61.9	61.61	86.88

TABLE 6. Ablation Study 2: Altering Loss Function for different Optimizers.

Optimizer	Loss Function	Average Accuracy(%)	Average Precision (%)	Average Recall (%)	Average F1 Score (%)	Average AUC (%)
Adam	Categorical Cross Entropy	89.8	90.02	89.8	89.76	98.34
	Mean Square Error	88.4	88.7	88.4	88.36	98.06
	Hinge Loss	33.8	11.51	33.8	17.15	50
Nadam	**Categorical Cross Entropy**	**91.5**	**91.69**	**91.5**	**91.48**	**98.94**
	Mean Square Error	91.2	91.5	91.2	91.2	98.07
	Hinge Loss	33.8	11.51	33.8	17.15	50

TABLE 7. Ablation study 3: Altering flatten layer for different optimizers.

Optimizer	Layers	Average Accuracy(%)	Average Precision (%)	Average Recall (%)	Average F1 Score (%)	Average AUC (%)
Adam	Flatten	89.8	90.02	89.8	89.76	98.34
	Global Average Pooling 2D	79.4	79.98	79.4	79.38	94.11
	Global Max Pooling 2D	82.9	83.95	82.9	82.98	96.72
Nadam	**Flatten**	**91.5**	**91.69**	**91.5**	**91.48**	**98.94**
	Global Average Pooling 2D	73.5	76.08	73.5	72.9	92.74
	Global Max Pooling 2D	88.2	88.54	88.2	88.2	98.12

TABLE 8. Ablation study 4: Altering attention module.

Attention Type	Average Accuracy(%)	Average Precision (%)	Average Recall (%)	Average F1 Score (%)	Average AUC (%)
Conv Block + without attention	89	89.55	89	88.94	98.5
Conv Block+CBAM [13]	90.7	91.5	90.7	90.7	98.61
Conv Block+SE [49]	90.4	90.69	90.4	90.35	98.66
Conv Block+LGAM (Lung-AttNet)	**91.5**	**91.69**	**91.5**	**91.48**	**98.94**

Turning into Adam optimizer, a similar trend of performance is visible. Lung-AttNet performed better when the learning rate was 0.001, which accounted for 89.8% average accuracy. However, the performance declined when the learning rate was 0.00001 with an average accuracy of 61.5%.

Besides, the research was performed by altering the loss functions reflected in TABLE 6. Keeping the Nadam optimizer constant, when Categorical Cross Entropy was used as a loss function, Lung-AttNet, obtained the highest performance with an average accuracy of 91.5%.A similar performance was observed for the Mean Square Error. However, in the case of the Hinge loss, the proposed performed worst in

all evaluation metrics. Additionally, the research was experimented with changing the flatten layer shown in TABLE 7. Keeping the Adam optimizer constant, it is observed that including flatten layer with the proposed model highlighted decent performance with an average accuracy and precision of 89.8% and 90.02% respectively. This accuracy was decreased by around 10% when Global Average Pooling 2D was incorporated.

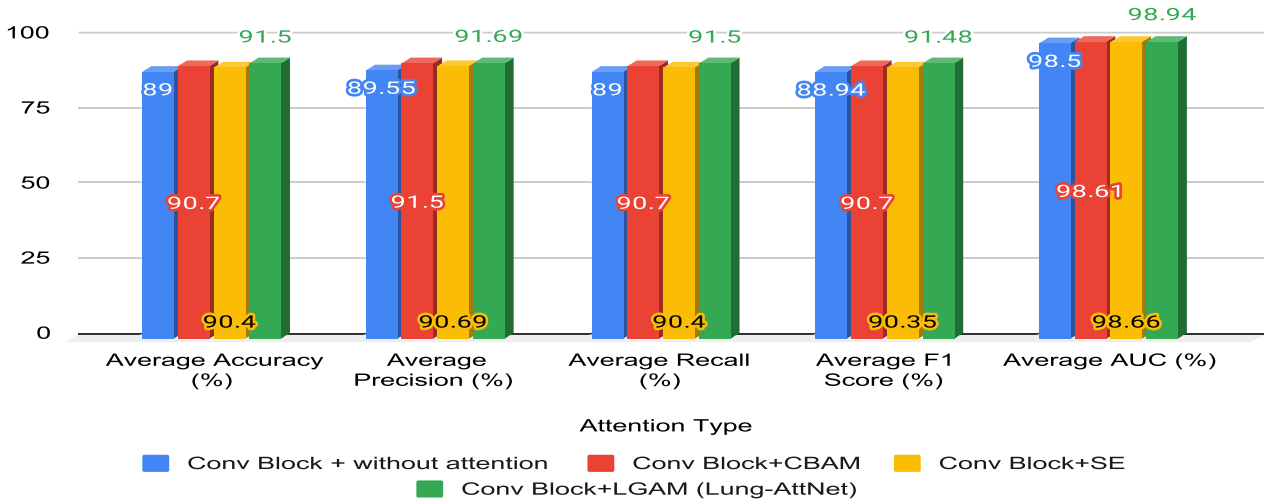

FIGURE 13. Comparison with SOTA attention mechanism.

TABLE 9. Model's parameters and sizes.

Model	Parameters	Model Size	Average Training Time Per Fold
Proposed Lung-AttNet	**3.749 M**	**43 MB**	**6.7 min**
AlexNet	22.6 M	247.3 MB	7.7 min
ResNet50	24.16 M	96.8 MB	9.91 min
InceptionV3	22.36 M	90.2 MB	9.7 min

In the case of the Nadam optimizer, incorporating Global Max Pooling 2D in place of flatten layer showed decent performance with an average accuracy of 88.2%.This accuracy fell by nearly 15% for Global Average Pooling 2D. Incorporating flatten layer with the proposed model illustrated the best performance with an average accuracy, precision, and recall of 91.5%, 91.69%, and 91.5% respectively.

The research was further conducted by altering the attention module shown in TABLE 8 and Figure. 13 respectively. It is visible that including LGAM with the model showed the best performance in all evaluation metrics. Besides, when the CBAM module was integrated with the conv block, the model's performance was decent, with an average accuracy of 90.7%. A similar performance was also observed for the Squeeze and Excitation (SE) block. The performance of the proposed model without attention block was below 90% in all evaluation metrics except AUC.

The performance of the proposed Lung-Attnet model with several transfer learning models in 5-fold cross-validation is demonstrated in Figure. 14. The proposed Lung-AttNet accounted for 91.5% accuracy on average being higher than Resnet50, and InceptionV3 by around 16% and 10% respectively. The average precision of Resnet50 and InceptionV3 were 76.82% and 83.48% respectively. Among different transfer learning models, the performance of the Alexnet was lowest having an average accuracy of 62%. Also, Lung-AttNet is faster in terms of computation and lighter in terms of model parameters (3.749 M), size (43 MB) compared to AlexNet, ResNet50 and InceptionV3 shown in TABLE 9.

The performance of our proposed model compared to related study methods used in the same dataset is shown in TABLE 10. It is visible from the table that our proposed model outperformed the state-of-the-art methods.

The proposed Lung-AttNet performance in a federated learning environment is illustrated in TABLE 11. In the federated learning environment, the experiment was carried out with different numbers of clients in 10 communication rounds and the number of test data was selected 100. It is visible that the proposed model achieved a global accuracy of 92% after 10 communication rounds while the number of clients was 2. Besides, it got a precision and F1 score of 92.27% and 92.03% respectively. Moreover, the AUC score was close to 99%. This accuracy remained constant (92%) when the client number was 3. The global accuracy decreased by 10% when the number of clients increased to 4. Further, 82.02% precision was achieved. The model got an accuracy of 67% when the client number was 5. Furthermore, it achieved 69.9% precision and 65.8% F1 score while dealing with 5 clients. These results are reflected in the confusion matrix shown in Figure. 16, Figure. 17, Figure. 18, and Figure. 19 respectively for different numbers of clients.

The global model's accuracy with respect to the communication round in different numbers of clients is shown in Figure. 15. It is clear that the global accuracy gradually increased with the increment of communication round. Finally, global accuracy reached 92% when the number of clients was 2 and 3. In case of number of the clients is 4, despite some fluctuation, there is a sharp rise in global accuracy with the increase of communication round and it grew to 82% accuracy at the end. When the number of clients is 5, it is observed that global accuracy remained constant till 4th communication round. After that, this figure slowly increased and at the end, it reached 67% accuracy.

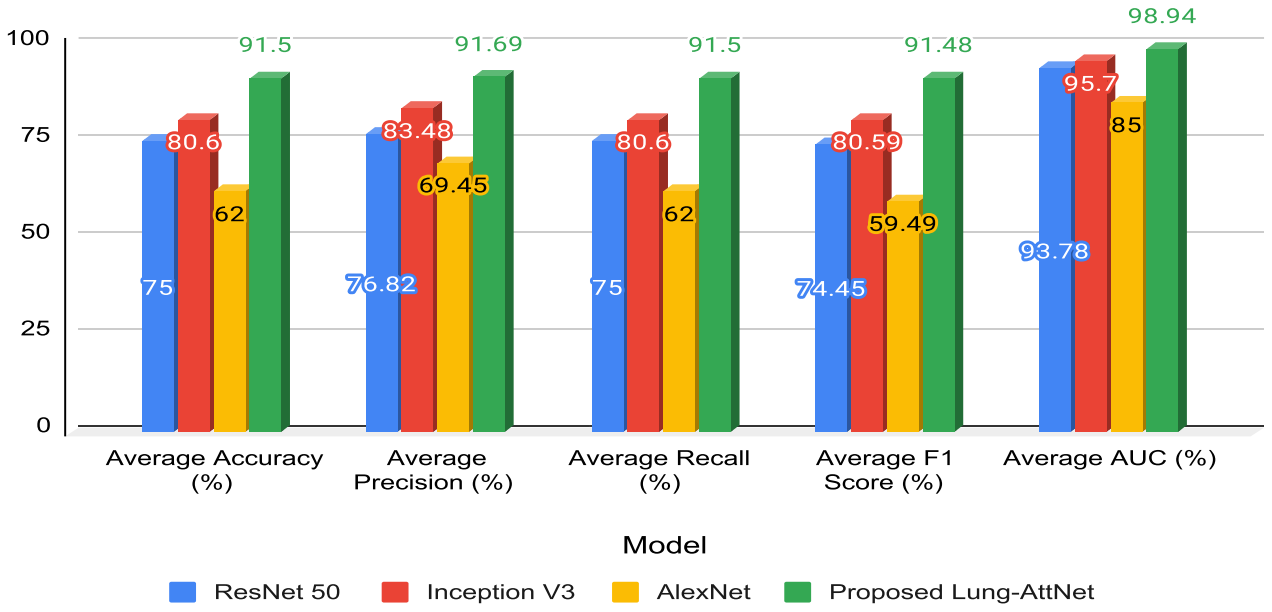

FIGURE 14. Performance comparison between transfer learning models and proposed Lung-AttNet in 5-fold cross-validation.

TABLE 10. Comparision with the related study methods on the same dataset in centralized environment.

Study	Method	Accuracy(%)	Precision (%)	Recall (%)	F1 Score (%)	AUC (%)
Mamun et al. [22]	Xception	82.1	-	82.02	-	90
Xu [20]	LeNet	63.78	-	-	-	-
Vij et al. [21]	VGG 16	77.62	60.38	30.48	40.67	75.08
Dadgar et al. [50]	InceptionResNetV2	91.1	84.9	-	81.5	95.8
Bhola et al. [51]	EfficientNet B2	90.16	91.28	90.16	90.09	-
This Study	**Lung-AttNet**	**91.5**	**91.69**	**91.5**	**91.48**	**98.94**

TABLE 11. Performance of the proposed model in Federated Learning environment.

Number of Clients	Acccuracy (%)	Precision (%)	Recall (%)	F1 Score (%)	AUC (%)
2	92	92.27	92	92.03	98.43
3	92	92.63	92	92.12	98.36
4	82	82.02	82	81.97	95.15
5	67	69.9	67	65.8	90.66

The proposed Lung-AttNet has the potential to assist clinical practitioners in detecting lung cancer at earlier stages, potentially improving patient outcomes. Besides, automating preliminary screening can reduce medical professionals' workload, allowing them to focus on complex cases. Moreover, implementing computer vision-based screening could lower healthcare costs by reducing additional medical testing. Currently, the proposed model is evaluated on a single dataset. There is much scope to implement the model on more diverse datasets. Also, for improving model performance and evaluating the effectiveness of the model in real-life scenarios prospective validation studies can be processed to assess the model's effectiveness in clinical trials. Also, in a distributed learning environment the model could be implemented.

A. XAI FOR MODEL EXPLAINABILITY

Due to the expansion of black box models, the need for model explainability has become more critical than ever. Hence, the importance of model explainability has grown significantly. Explainable AI (XAI) techniques are pivotal in providing the model's interpretability and making the model trustworthy. By improving interpretability, in medical imaging, XAI fosters trust among users and helps debug models, ensure fairness, and comply with regulatory requirements.

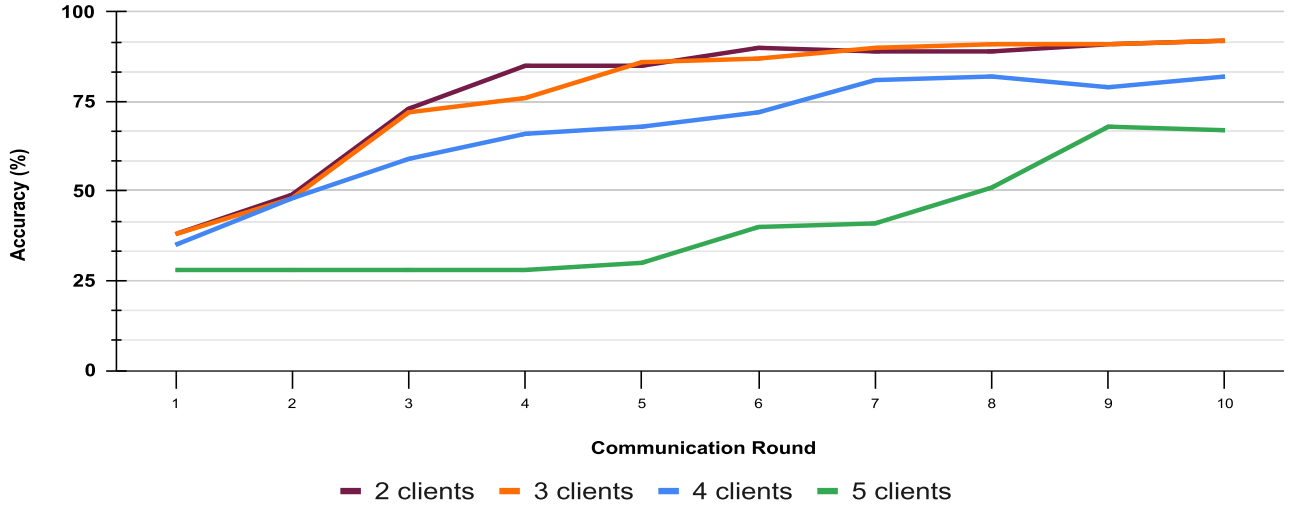

FIGURE 15. Accuracy versus communication round for different number of clients.

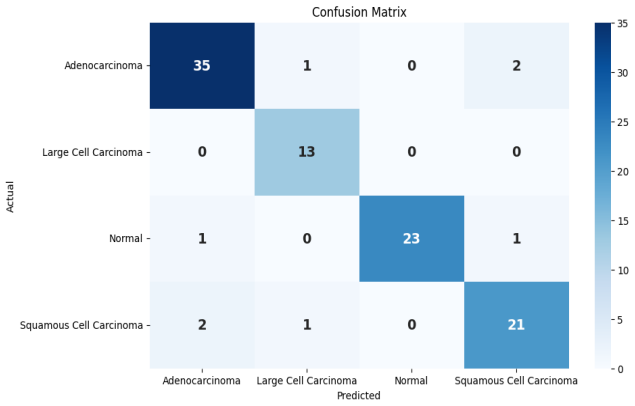

FIGURE 16. Confusion matrix for 2 clients.

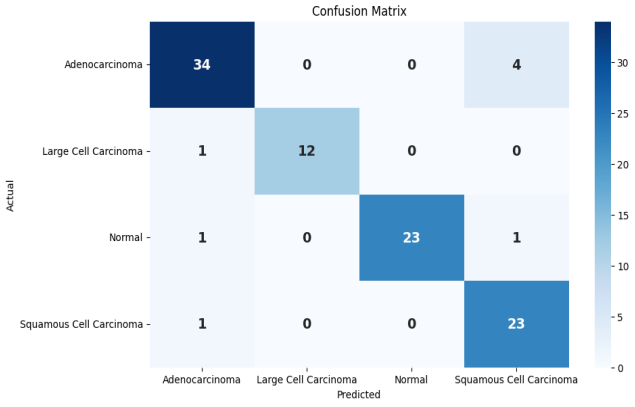

FIGURE 17. Confusion matrix for 3 clients.

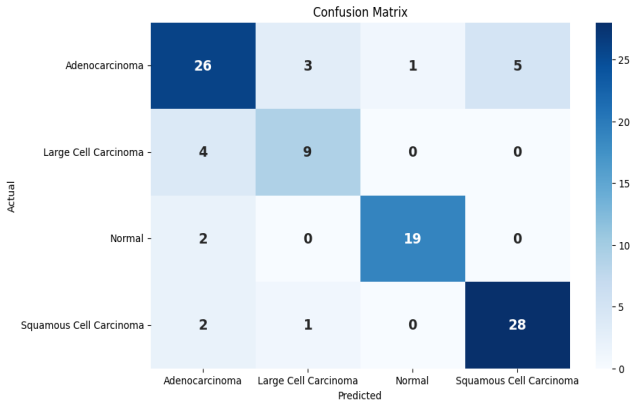

FIGURE 18. Confusion matrix for 4 clients.

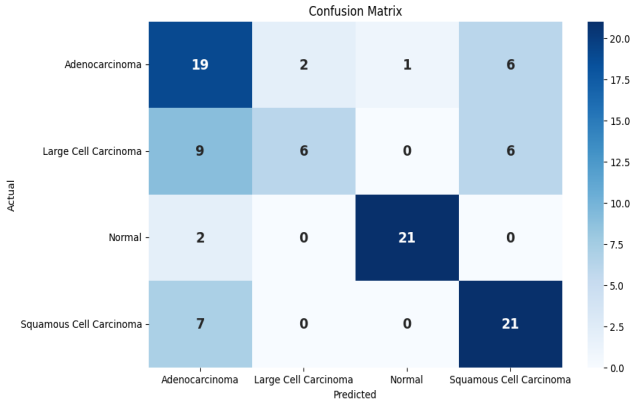

FIGURE 19. Confusion matrix for 5 clients.

A common XAI method, LIME [51] is a model agnostic that treats each deep learning model as a black box. To provide a visual explanation of the model's prediction, LIME does not require any access of inner layers. By creating marked boundaries for individual input images, LIME provides interpretability of the prediction of the image rather than the model's behaviour. The yellow marked bounded areas in Figure. 20, Figure. 21, Figure. 22, and Figure. 23

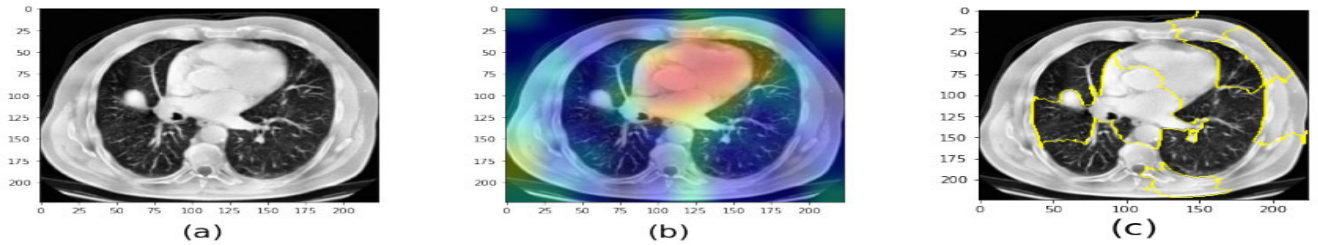

FIGURE 20. Grad-CAM and LIME interpretation for Adenocarcinoma: (a), (b), (c) represent Original, Grad-CAM, LIME respectively.

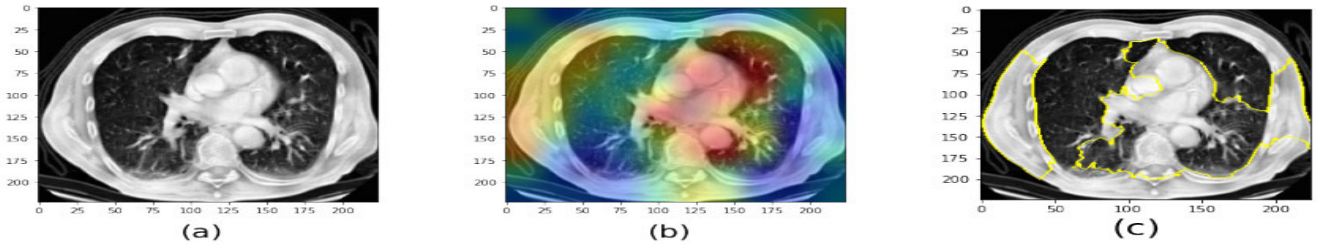

FIGURE 21. Grad-CAM and LIME interpretation for Large Cell Carcinoma: (a), (b), (c) represent Original, Grad-CAM, LIME respectively.

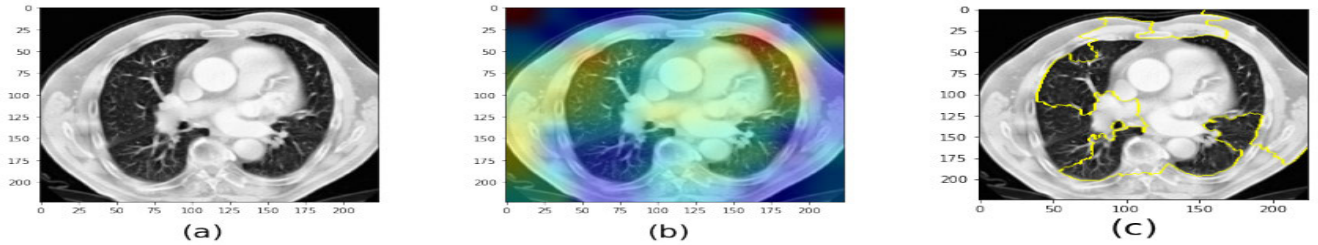

FIGURE 22. Grad-CAM and LIME interpretation for Squamous Cell Carcinoma: (a), (b), (c) represent Original, Grad-CAM, LIME respectively.

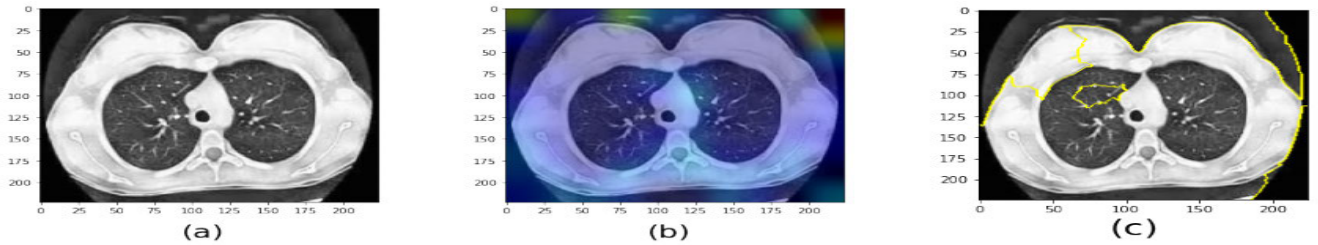

FIGURE 23. Grad-CAM and LIME interpretation for Normal: (a), (b), (c) represent Original, Grad-CAM, LIME respectively.

ensure the regions that are responsible for the model's prediction.

Compared to LIME, Grad-CAM [52] is a model interpretability technique that generates heat maps to figure out the important regions of the input image in the prediction of the target class. To generate a heat map (Grad-CAM), gradient information of the target class flows to the last convolution layer. As the last convolution layer of the network contains detailed information in spatial dimensions, it assigns importance to decision-making. The interpretable regions in the heat map with colors ranging from blue to red are shown in Figure. 20, Figure. 21, Figure. 22, and Figure. 23. The red zone defines the most important region of the class for decision-making whereas blue is the least important.

VI. CONCLUSION

Lung cancer is the deadliest among all cancers for which early diagnosis is crucial for increasing the survival of the patient. CT scan images are preferred for lung cancer

diagnosis by physicians. Therefore, this study will provide a solution by making an automated lung cancer diagnosis system using CT scan images. This research proposed a novel attention mechanism-based lung cancer detection model called Lung-AttNet. The experimentation was conducted on both centralized and Federated Learning environments utilizing the Kaggle CT Scan dataset. Federated Learning helps ensure the privacy and protection of patient data. In performance analysis, it was observed that the proposed model outperformed the SOTA models on the same dataset. Finally, the XAI methods such as LIME and Grad-CAM were integrated to provide the visual interpretability of the results. In the future, the proposed model can be improved by deploying on different datasets. Also, to boost the robustness of the model, adversarial training can be performed by training the model on adversarial examples. Furthermore, techniques such as differential privacy and blockchain mechanisms can be utilized to strengthen privacy measures.

ACKNOWLEDGMENT

(Chamak Saha and Somak Saha are co-first authors.)

REFERENCES

[1] S. Akila Agnes, A. Arun Solomon, and K. Karthick, "Wavelet U-Net++ for accurate lung nodule segmentation in CT scans: Improving early detection and diagnosis of lung cancer," *Biomed. Signal Process. Control*, vol. 87, Jan. 2024, Art. no. 105509.

[2] A. Singareddy, M. E. Flanagan, P. Samson, S. N. Waqar, S. Devarakonda, J. P. Ward, B. H. Herzog, A. Rohatgi, C. G. Robinson, F. Gao, R. Govindan, V. Puri, and D. Morgensztern, "Trends in stage i lung cancer," *Clin. Lung Cancer*, vol. 24, no. 2, pp. 114–119, Nov. 2022.

[3] N. S. Nadkarni and S. Borkar, "Detection of lung cancer in CT images using image processing," in *Proc. 3rd Int. Conf. Trends Electron. Informat. (ICOEI)*, Apr. 2019, pp. 863–866.

[4] A. Chaudhary and S. S. Singh, "Lung cancer detection on CT images by using image processing," in *Proc. Int. Conf. Comput. Sci.*, Sep. 2012, pp. 142–146.

[5] B. Cherradi, O. Terrada, A. Ouhmida, S. Hamida, A. Raihani, and O. Bouattane, "Computer-aided diagnosis system for early prediction of atherosclerosis using machine learning and K-fold cross-validation," in *Proc. Int. Congr. Adv. Technol. Eng. (ICOTEN)*, Jul. 2021, pp. 1–9.

[6] H.-C. Shin, H. R. Roth, M. Gao, L. Lu, Z. Xu, I. Nogues, J. Yao, D. Mollura, and R. M. Summers, "Deep convolutional neural networks for computer-aided detection: CNN architectures, dataset characteristics and transfer learning," *IEEE Trans. Med. Imag.*, vol. 35, no. 5, pp. 1285–1298, May 2016.

[7] S. H. Hosseini, R. Monsefi, and S. Shadroo, "Deep learning applications for lung cancer diagnosis: A systematic review," *Multimedia Tools Appl.*, vol. 83, no. 5, pp. 14305–14335, Jul. 2023.

[8] S. K. Thakur, D. P. Singh, and J. Choudhary, "Lung cancer identification: A review on detection and classification," *Cancer Metastasis Rev.*, vol. 39, no. 3, pp. 989–998, Sep. 2020.

[9] T. K. Dutta, D. R. Nayak, and Y.-D. Zhang, "ARM-net: Attention-guided residual multiscale CNN for multiclass brain tumor classification using MR images," *Biomed. Signal Process. Control*, vol. 87, Jan. 2024, Art. no. 105421.

[10] D. Truhn et al., "Encrypted federated learning for secure decentralized collaboration in cancer image analysis," *Med. Image Anal.*, vol. 92, Feb. 2024, Art. no. 103059.

[11] H. Guan, P.-T. Yap, A. Bozoki, and M. Liu, "Federated learning for medical image analysis: A survey," *Pattern Recognit.*, vol. 151, Jul. 2024, Art. no. 110424.

[12] Md. N. Hossen, V. Panneerselvam, D. Koundal, K. Ahmed, F. M. Bui, and S. M. Ibrahim, "Federated machine learning for detection of skin diseases and enhancement of Internet of Medical Things (IoMT) security," *IEEE J. Biomed. Health Informat.*, vol. 27, no. 2, pp. 835–841, Feb. 2023.

[13] S. Woo, J. Park, J. Lee, and I. S. Kweon, "CBAM: Convolutional block attention module," in *Proc. Eur. Conf. Comput. Vis. (ECCV)*, Jan. 2018, pp. 3–19.

[14] V. Jindal, V. Kukreja, D. P. Singh, S. Vats, and S. Mehta, "Modernizing lung cancer detection: The federated learning CNN approach," in *Proc. 4th IEEE Global Conf. Advancement Technol. (GCAT)*, Oct. 2023, pp. 1–6.

[15] M. Toğaçar, B. Ergen, and Z. Cömert, "Detection of lung cancer on chest CT images using minimum redundancy maximum relevance feature selection method with convolutional neural networks," *Biocybernetics Biomed. Eng.*, vol. 40, no. 1, pp. 23–39, Jan. 2020.

[16] R. Chitale, B. Shah, S. Bhalgat, A. Pandey, and S. A. Jakhete, "Utilization of CNN and ensemble methods to support medical practitioners in categorizing lung cancer: A research paper," in *Proc. 7th Int. Conf. Comput., Commun., Control Autom. (ICCUBEA)*, Aug. 2023, pp. 1–5.

[17] F. Al-Areqi, A. T. Çelebi, and M. Z. Konyar, "Lung cancer classification using image enhancement and CNN-based pre-trained models," in *Proc. Innov. Intell. Syst. Appl. Conf. (ASYU)*, Oct. 2023, pp. 1–7.

[18] M. Šaric, M. Russo, M. Stella, and M. Sikora, "CNN-based method for lung cancer detection in whole slide histopathology images," in *Proc. 4th Int. Conf. Smart Sustain. Technol. (SpliTech)*, Jun. 2019, pp. 1–4.

[19] H. F. Al-Yasriy, M. S. AL-Husieny, F. Y. Mohsen, E. A. Khalil, and Z. S. Hassan, "Diagnosis of lung cancer based on CT scans using CNN," *Proc. IOP Conf. Ser., Mater. Sci. Eng.*, vol. 928, Nov. 2020, Art. no. 022035.

[20] H. Xu, "Comparison of CNN models in non-small lung cancer diagnosis," in *Proc. IEEE 3rd Int. Conf. Power, Electron. Comput. Appl. (ICPECA)*, Jan. 2023, pp. 1169–1174.

[21] A. Vij and K. S. Kaswan, "Prediction of lung cancer using convolution neural networks," in *Proc. Int. Conf. Artif. Intell. Smart Commun. (AISC)*, Jan. 2023, pp. 737–741.

[22] M. Mamun, M. I. Mahmud, M. Meherin, and A. Abdelgawad, "LCD-ctCNN: Lung cancer diagnosis of CT scan images using CNN based model," in *Proc. 10th Int. Conf. Signal Process. Integr. Netw. (SPIN)*, Mar. 2023, pp. 205–212.

[23] W. Abdul, "An automatic lung cancer detection and classification (ALCDC) system using convolutional neural network," in *Proc. 13th Int. Conf. Develop. eSyst. Eng. (DeSE)*, Dec. 2020, pp. 443–446.

[24] T. Sajja, R. Devarapalli, and H. Kalluri, "Lung cancer detection based on CT scan images by using deep transfer learning," *Traitement du Signal*, vol. 36, no. 4, pp. 339–344, Oct. 2019.

[25] A. Bhola, D. V. Kiran, D. G. A. Ram, N. Vrajesh, and A. Tiwari, "Lung cancer detection using transfer learning and EfficientNet B2 architecture," in *Proc. Int. Conf. Disruptive Technol. (ICDT)*, May 2023, pp. 395–400.

[26] K. R. Lathakumari, A. C. Ramachandra, U. C. Avanthi, C. Basil Ronald, and T. Bhavatharani, "Classification of non-small cell lung cancer using deep learning," in *Proc. Int. Conf. Appl. Intell. Sustain. Comput. (ICAISC)*, Jun. 2023, pp. 1–5.

[27] A. A. Shah, H. A. M. Malik, A. Muhammad, A. Alourani, and Z. A. Butt, "Deep learning ensemble 2D CNN approach towards the detection of lung cancer," *Sci. Rep.*, vol. 13, no. 1, p. 2987, Feb. 2023.

[28] A. K. Swain, A. Swetapadma, J. K. Rout, and B. K. Balabantaray, "Classification of non-small cell lung cancer types using sparse deep neural network features," *Biomed. Signal Process. Control*, vol. 87, Jan. 2024, Art. no. 105485.

[29] M. Q. Shatnawi, Q. Abuein, and R. Al-Quraan, "Deep learning-based approach to diagnose lung cancer using CT-scan images," *Intell.-Based Med.*, vol. 11, Jan. 2025, Art. no. 100188.

[30] S. Hangaragi, N. Neelima, V. Venugopal, S. Ganguly, J. Mudi, and J.-H. Choi, "CAE SynthImgGen: Revolutionizing cancer diagnosis with convolutional autoencoder-based synthetic image generation," *Alexandria Eng. J.*, vol. 115, pp. 343–354, Mar. 2025.

[31] D. Mhaske, K. Rajeswari, and R. Tekade, "Deep learning algorithm for classification and prediction of lung cancer using CT scan images," in *Proc. 5th Int. Conf. Comput., Commun., Control Autom. (ICCUBEA)*, Sep. 2019, pp. 1–5.

[32] M. K. Islam, M. M. Rahman, M. S. Ali, S. M. Mahim, and M. S. Miah, "Enhancing lung abnormalities detection and classification using a deep convolutional neural network and GRU with explainable AI: A promising approach for accurate diagnosis," *Mach. Learn. Appl.*, vol. 14, Dec. 2023, Art. no. 100492.

[33] V. R. Nitha and S. S. V. Chandra, "An eXplainable machine learning framework for predicting the impact of pesticide exposure in lung cancer prognosis," *J. Comput. Sci.*, vol. 84, Jan. 2025, Art. no. 102476.

[34] T. Gulsoy and E. Baykal Kablan, "FocalNeXt: A ConvNeXt augmented FocalNet architecture for lung cancer classification from CT-scan images," *Expert Syst. Appl.*, vol. 261, Feb. 2025, Art. no. 125553.

[35] V. Jindal, V. Kukreja, D. P. Singh, S. Vats, and S. Mehta, "Embracing federated learning and CNN for distributed diagnosis of lung diseases: A novel approach," in *Proc. Int. Conf. Comput., Commun., Intell. Syst. (ICCCIS)*, Nov. 2023, pp. 122–127.

[36] V. Jindal, V. Kukreja, D. P. Singh, S. Vats, and S. Mehta, "Pushing diagnostic frontiers: Federated learning CNN for diverse lung disease," in *Proc. 4th IEEE Global Conf. Advancement Technol. (GCAT)*, Oct. 2023, pp. 1–6.

[37] M. K. Islam, M. M. Rahman, M. S. Ali, S. M. Mahim, and M. S. Miah, "Enhancing lung abnormalities diagnosis using hybrid DCNN-ViT-GRU model with explainable AI: A deep learning approach," *Image Vis. Comput.*, vol. 142, Feb. 2024, Art. no. 104918.

[38] M. I. Adnan Palash and M. A. Yousuf, "A federated learning-based model for the detection of lung cancer from CT scan images," in *Proc. 6th Int. Conf. Electr. Eng. Inf. Commun. Technol. (ICEEICT)*, May 2024, pp. 741–745.

[39] M. Field, S. Vinod, G. P. Delaney, N. Aherne, M. Bailey, M. Carolan, A. Dekker, S. Greenham, E. Hau, J. Lehmann, J. Ludbrook, A. Miller, A. Rezo, J. Selvaraj, J. Sykes, D. Thwaites, and L. Holloway, "Federated learning survival model and potential radiotherapy decision support impact assessment for non–small cell lung cancer using real-world data," *Clin. Oncol.*, vol. 36, no. 7, pp. e197–e208, Jul. 2024.

[40] A. Heidari, D. Javaheri, S. Toumaj, N. J. Navimipour, M. Rezaei, and M. Unal, "A new lung cancer detection method based on the chest CT images using federated learning and blockchain systems," *Artif. Intell. Med.*, vol. 141, Jul. 2023, Art. no. 102572.

[41] L. Liu, K. Fan, and M. Yang, "Federated learning: A deep learning model based on resnet18 dual path for lung nodule detection," *Multimedia Tools Appl.*, vol. 82, no. 11, pp. 17437–17450, May 2023.

[42] G. Mostafa, M. S. Hamidi, and D. M. Farid, "Detecting lung cancer with federated and transfer learning," in *Proc. 26th Int. Conf. Comput. Inf. Technol. (ICCIT)*, Dec. 2023, pp. 1–6.

[43] M. M. Hossain, M. F. Ahamed, M. R. Islam, and M. R. Imam, "Privacy preserving federated learning for lung cancer classification," in *Proc. 26th Int. Conf. Comput. Inf. Technol. (ICCIT)*, Dec. 2023, pp. 1–6.

[44] F. F. Babar, F. Jamil, T. Alsboui, F. F. Babar, S. Ahmad, and R. I. Alkanhel, "Federated active learning with transfer learning: Empowering edge intelligence for enhanced lung cancer diagnosis," in *Proc. Int. Wireless Commun. Mobile Comput. (IWCMC)*, May 2024, pp. 1333–1338.

[45] *Chest CT-scan Images Dataset—kaggle.com*. Accessed: Aug. 8, 2023. [Online]. Available: https://www.kaggle.comdatasets/mohamedhanyyy/chest-ctscan-images

[46] Y. L. Khaleel, M. A. Habeeb, and H. Alnabulsi, "Adversarial attacks in machine learning: Key insights and defense approaches," *Appl. Data Sci. Anal.*, vol. 2024, pp. 121–147, Aug. 2024.

[47] M. Dölarslan, "CRISPR-Cas9 mediated gene correction of CFTR mutations in cystic fibrosis: Evaluating efficacy, safety, and long-term outcomes in patient-derived lung organoids," *SHIFAA*, vol. 2023, pp. 41–47, May 2023.

[48] S. Majumder, N. Gautam, A. Basu, A. Sau, Z. W. Geem, and R. Sarkar, "MENet: A mitscherlich function based ensemble of CNN models to classify lung cancer using CT scans," *PLoS ONE*, vol. 19, no. 3, Mar. 2024, Art. no. e0298527.

[49] J. Hu, L. Shen, and G. Sun, "Squeeze-and-Excitation networks," in *Proc. IEEE/CVF Conf. Comput. Vis. Pattern Recognit.*, Jun. 2018, pp. 7132–7141.

[50] S. Dadgar and M. Neshat, "Comparative hybrid deep convolutional learning framework with transfer learning for diagnosis of lung cancer," in *Proc. Int. Conf. Soft Comput. Pattern Recognit.*, Jan. 2023, pp. 296–305.

[51] M. T. Ribeiro, S. Singh, and C. Guestrin, "'Why should I trust you?' Explaining the predictions of any classifier," in *Proc. 22nd ACM SIGKDD Int. Conf. Knowl. Discovery Data Mining*, 2016, pp. 1135–1144.

[52] R. R. Selvaraju, M. Cogswell, A. Das, R. Vedantam, D. Parikh, and D. Batra, "Grad-CAM: Visual explanations from deep networks via gradient-based localization," in *Proc. IEEE Int. Conf. Comput. Vis. (ICCV)*, Oct. 2017, pp. 618–626.

CHAMAK SAHA received the B.Sc. degree in computer science and engineering from BRAC University, Bangladesh, in 2023. He is currently pursuing the M.S. degree in animal and dairy science at the University of Georgia, USA, with a focus on computer vision and precision livestock science. His research experience lies in computer vision and applied machine learning. His research interests include applied artificial intelligence, particularly in precision livestock science, agricultural automation, biomedical image processing, healthcare informatics, and business analytics. He is also interested in federated learning and adversarial machine learning.

SOMAK SAHA received the B.Sc. degree from the Department of Computer Science and Engineering (CSE), BRAC University, Dhaka, in 2023. He has research experience in the arena of agricultural automation. Currently, he is working on multiple research projects in applied machine learning, deep learning, and computer vision. His research interests include federated learning, adversarial machine learning, biomedical image processing, and healthcare informatics.

MD. ASADUR RAHMAN (Student Member, IEEE) received the B.Sc. and M.Sc. degrees from the Department of Electrical and Electronic Engineering, KUET, Bangladesh, in 2012 and 2014, respectively, and the Ph.D. degree from the Department of Biomedical Engineering, KUET, in 2020. He is currently an Assistant Professor in the Department of Biomedical Engineering, Military Institute of Science and Technology, Dhaka, Bangladesh. His research interests include neuroimaging, brain–computer interface, intelligent algorithms, and machine learning.

MD. MAHMUDUL HAQUE MILU received the B.Sc. degree in biomedical engineering from Khulna University of Engineering and Technology, Bangladesh, and the M.S. degree in biomedical physics and technology from the University of Dhaka, Bangladesh. He is currently an Assistant Professor with the Department of Biomedical Engineering, Jashore University of Science and Technology, Bangladesh. His research interests include polymeric biomaterials, regenerative medicine, drug delivery, wound healing, electrospinning, biosignal processing, and bio-optics.

HIROKI HIGA received the Ph.D. degree in electronics engineering from Tohoku University, Japan, in 1997. Since 1997, he has been with the Department of Electric and Electronics Engineering, University of the Ryukyus, where he is currently a Professor with the Faculty of Engineering, Electrical and Systems Engineering Program. From 2008 to 2009, and 2016, he was a Visiting Researcher with Old Dominion University, Norfolk, VA, USA. His research interests include robotics and biomedical engineering.

MOHD ABDUR RASHID received the Ph.D. degree in electrical and information engineering from the University of the Ryukyus, Japan. He is currently a Professor with the Department of Electrical and Electronic Engineering (EEE), Noakhali Science and Technology University, Bangladesh. Besides, he has work experience in Malaysia as a Faculty Member for six years, and in Japan and Canada as a Postdoctoral Fellow for three years. He has authored more than 97 technical papers in journals and conferences. His research interests include multidisciplinary fields, including mathematical modeling, electronic devices, and biomedical engineering.

NASIM AHMED (Senior Member, IEEE) received the M.Sc. degree in computer engineering from Universiti Malaysia Perlis, Malaysia, in 2009, and the Ph.D. degree in computer science from Massey University, New Zealand, in 2022. His research interests include data science applications in healthcare and agriculture, big data clusters, artificial intelligence's role in education (specifically policymaking and industry), and data security.